Vol 15 No 8, August 2006
1009-1963/2006/15(08)/1731-07

Chinese Physics

© 2006 Chin. Phys. Soc.
and IOP Publishing Ltd

In-line phase contrast for weakly absorbing materials with a microfocus x-ray source*

Zhang Di(章　迪)†, Li Zheng(李　政), Huang Zhi-Feng(黄志峰),
Yu Ai-Min(禹爱民), and Sha Wei(沙　薇)

Department of Engineering Physics, Tsinghua University, Beijing 100084, *China*

(Received 9 December 2005; revised manuscript received 22 April 2006)

For weakly absorbing materials, image contrast can be enhanced by phase contrast in formation. The effectiveness of the in-line phase contrast technique relies on its ability to record intensity data which contain information on the x-ray's phase shift. Four kinds of approaches to the relationship between intensity distribution and phase shift are reviewed and discussed. A micro-focal x-ray source with high geometrical magnification is used to acquire phase contrast images. A great improvement on image quality is shown and geometrical parameters are modified for comparison between different imaging positions.

Keywords: in-line phase contrast, intensity distribution, microfocus, Fresnel diffraction
PACC: 0785, 4230K

1. Introduction

X-ray beams, as a kind of electromagnetic wave, have both intensity and phase variations when passing through objects. Since x-rays were discovered in 1895 by Roentgen, their property of attenuation has been used, especially as a major means of clinical nondestructive diagnosis, as well as in industry and material science research. Meanwhile, applications of the phase effects of x-rays developed much slowly. Since phase contrast microscopy was invented by Zernike in 1935[1] and holography was suggested by Gabor in 1948,[2] no specific use of x-ray phase effects had occurred until after the Gottingen group's contributions to transmission x-ray microscopy (TXM)[3] for detecting the phase φ by Zernike phase contrast, and Morrison's research on scanning transmission x-ray microscopy (STXM)[4,5] for detecting the local phase gradient ∇_{φ}. However, these techniques are applicable only in the soft x-ray region. For imaging with hard x-rays, only in recent years have several new techniques been developed, such as interferometric methods by Momose,[6] diffraction enhanced imaging (DEI) by Wilkins[7,8] and Chapman,[9,10] and the in-line method by Wilkins,[11] Snigirev[12] and Cloetens,[13] which are used to measure φ, ∇_{φ} and ∇^2_{φ}, respectively. Since these techniques do not rely on absorption that serves as the contrast mechanism, they are applicable to weakly absorbing objects, in which the conventional x-ray imaging method cannot work well. For the imaging of biological soft tissue, such as tumours, blood vessels, and low absorption materials, phase contrast imaging is a powerful means of improving image quality. In 1996 a significant advance was made in the field of in-line phase contrast imaging by Gureyev and Wilkins, who proved mathematically that a source generating spherical wave incidence could also be used, as long as its spatial coherence is high. Moreover, the possibility of using a polychromatic x-ray source was suggested.[11,18] Based on these developments, microfocus x-rays would be a useful source for in-line phase contrast imaging. In the past, the incoherence of time resolution and spatial resolution were discussed and a mechanism for imaging under parallel beams was analysed in Fourier form.[14,19] In this paper, several ways of establishing the effectiveness of in-line phase contrast are discussed, the Fourier method using spherical waves in a microfocus x-ray source is suggested, and some experimental results are also presented and analysed.

2. Basic principle of phase contrast

The refractive index of a sample can be written as follows:

$$n = 1 - \delta - \mathrm{i}\beta. \tag{1}$$

*Project supported by the National Natural Science Foundation of China (Grant No 10475044).
†Corresponding author. E-mail: zhangdi00@mails.tsinghua.edu.cn

The transmission function of a sample is

$$\begin{aligned} q &= \exp\left(\int_z -k(\mathrm{i}\delta+\beta)\mathrm{d}z'\right) \\ &= \exp\left(-\mathrm{i}k\int_z \delta\mathrm{d}z' - k\int_z \beta\mathrm{d}z'\right) \\ &= \exp(\mathrm{i}\varphi+\mu). \end{aligned} \quad (2)$$

Here $k=2\pi/\lambda$; λ is the wavelength of the x-ray; φ is the phase shift mentioned above, and μ is the attenuation coefficient.

From what has been discussed above, clearly δ and β are the phase-shifting and absorption components, respectively.

A diagrammatic sketch of the imaging system is shown in Fig.1. The object is illuminated by a plane wave, and its wavefront shape varies with thickness and refractive index of the object. Both the object plane and image plan are perpendicular to the direction of propagation of the x-ray beam.

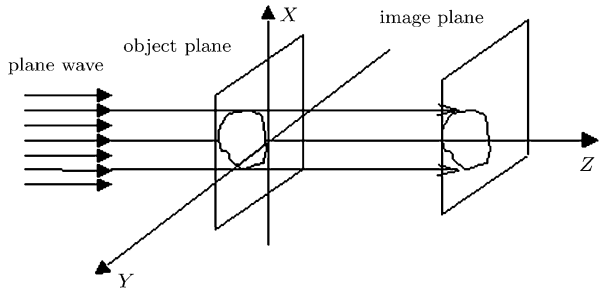


Fig.1. Diagrammatic sketch of in-line phase contrast imaging.

The most crucial factor that establishes the in-line phase contrast method as an effective imaging technique is the relationship between the intensity I in the image plane and the Laplacian of phase shift φ. In fact there are several ways, commonly based on the Fresnel integral, to establish this relationship. Four different ways will be discussed in the following.

2.1. Fourier form

According to Fresnel diffraction theory, when a plane wave reaches the sample equably, the wavefunction is

$$f(x,y)=\frac{\mathrm{i}}{\lambda}\iint q(X,Y)\cdot\frac{\exp(\mathrm{i}kr)}{r}\mathrm{d}X\mathrm{d}Y. \quad (3)$$

where $r=\sqrt{(x-X)^2+(y-Y)^2+z^2}$, z is the distance from the sample plane to the image plane. In the small angle approximation, after Taylor expansion, the one-dimensional form of Eq.(3) becomes[15]

$$\begin{aligned} f(x) &= \left(\frac{\mathrm{i}}{\lambda z}\right)^{1/2}\exp(\mathrm{i}kz) \\ &\quad\times\int q(X)\cdot\exp\left\{\frac{\mathrm{i}k(x-X)^2}{2z}\right\}\mathrm{d}X. \end{aligned} \quad (4)$$

Considering the definitions of convolution and Fourier transform, we can obtain

$$\begin{aligned} f(x) &= \exp(\mathrm{i}kz)\int Q(u)\exp\{-2\pi\mathrm{i}ux\} \\ &\quad\times\exp\{\mathrm{i}\pi z\lambda u^2\}\mathrm{d}u, \end{aligned} \quad (5)$$

where $Q(u)$ is the Fourier form of $q(x)$, and $\int Q(u)\exp\{-2\pi\mathrm{i}ux\}\exp\{\mathrm{i}\pi z\lambda u^2\}\mathrm{d}u$ is exactly the inverse Fourier transform (IFT) of $Q(u)\exp\{\mathrm{i}\pi z\lambda u^2\}$. If $\chi=\pi z\lambda u^2$ is small enough, we have $\sin\chi\approx\chi$. Then Eq.(5) becomes

$$\begin{aligned} f(x) &= \exp(\mathrm{i}kz)(q(x)+\mathrm{i}\pi z\lambda \\ &\quad\times\int u^2Q(u)\exp(-2\pi\mathrm{i}ux)\mathrm{d}u) \end{aligned} \quad (6)$$

for a pure phase object: $q(x)=\exp\{\mathrm{i}\varphi(x)\}$. Using the property of the Fourier Transform yields

$$\begin{aligned} f(x) &= \exp(\mathrm{i}kz)\exp(\mathrm{i}\varphi(x)) \\ &\quad\times\left(1+\frac{z\lambda}{4\pi}\varphi''(x)+\frac{\mathrm{i}z\lambda}{4\pi}\varphi'(x)^2\right). \end{aligned} \quad (7)$$

To the first order in $z\lambda$,[15] we have

$$I=\left|f(x)\right|^2\approx 1+\frac{z\lambda}{2\pi}\varphi''(x). \quad (8)$$

The phase shift φ reflects the phase variation of an x-ray passing through an object. Based on its relationship with φ, the intensity distribution I in the image plane can deduce the inner structure of the object.

2.2. New Fourier method

A new Fourier method was developed in 1997.[14] After IFT of Eq. (5), it becomes

$$F(u)=\exp\{\mathrm{i}kz\}Q(u)\exp\{\mathrm{i}\chi\}. \quad (9)$$

Then the image intensity becomes in Fourier space (2-Dimensional)

$$\begin{aligned} I(u,v) &= \delta(u,v)-2m(u,v)\cos\chi \\ &\quad -2\Phi(u,v)\sin\chi. \end{aligned} \quad (10)$$

where m and Φ are Fourier forms of μ and φ, respectively. For a weakly absorbing object, and in the same approximation as the above, Eq.(10) becomes

$$I(u,v)=\delta(u,v)-2\pi\lambda z(u^2+y^2)\Phi(u,y). \quad (11)$$

After IFT, in normal space, the intensity is[14]

$$I(x,y) = 1 - \frac{\lambda z}{2\pi}\nabla^2\varphi(x,y). \tag{12}$$

For a two–dimensional object, we can clearly see the relationship between intensity I in the image plane and the Laplacian of the phase shift φ.

2.3. Mutual intensity method

With the help of mutual intensity theory, another new model was established in 1999, with a partially coherent source taken into consideration.[17] Assume that the mutual intensity in the object plane is $J_{12}(x_1, y_1, x_2, y_2)$, the transmission function of the object is $q(X, Y)$, and the illuminated area is D. Let us define

$$T(X,Y) = \begin{cases} 1, & \text{outside object,} \\ q(X,Y), & \text{inside object.} \end{cases}$$

According to the mutual intensity propagation theory, the intensity in the image plane is given by:

$$I(x,y) = \iint\limits_D \mathrm{d}x_1\mathrm{d}y_1 \iint\limits_D J_{12}(x_1,y_1,x_2,y_2)\frac{1}{\lambda^2 d_1 d_2}\exp\{\mathrm{i}k(d_1-d_2\}T(x_1,y_1)T^*(x_2,y_2)\mathrm{d}x_2\mathrm{d}y_2, \tag{13}$$

where d_1 and d_2 are the distances from (x_1, y_1) and (x_2, y_2) to (x, y), respectively. In the paraxial approximation the above equation is analogous to the intensity distribution of a coherent in-line Gabor hologram with three terms.

If the source has a uniform circular shape with a radius of ρ, the mutual intensity $J_{12}(x_1, y_1, x_2, y_2)$ could be obtained from the Van Cittert–Zernike theorem. The approximation of the integral in Eq.(13) then becomes

$$\begin{aligned} I(x,y) = 2\mathrm{Re}[\int \mathrm{d}z \iint\limits_D (T(x_1,y_1,z)-1) \\ \times h(x,y,x_1,y_1,z)\mathrm{d}x_1\mathrm{d}y_1]. \end{aligned} \tag{14}$$

For weakly absorbing objects, the above equation becomes[17]

$$\begin{aligned} I(x,y) = 1 - 2\iint\limits_D \{\mu(x_1,y_1)\cos\{\frac{\pi}{\lambda z}[(x-x_1)^2+(y-y_1)^2]\}\}\mathrm{d}x_1\mathrm{d}y_1 - 2\iint\limits_D \{\varphi(x_1,y_1) \\ \times \sin\{\frac{\pi}{\lambda z}[(x-x_1)^2+(y-y_1)^2]\}\}\mathrm{d}x_1\mathrm{d}y_1. \end{aligned} \tag{15}$$

which is exactly the spatial form of Eq.(10). Thus, all conclusions drawn from New Fourier method could be confirmed here, including the relationship between distribution of I in the image plane and the Laplacian of phase shift φ.

2.4. Analytical method

In fact, the Fresnel integral could be directly analysed without the assistance of Fourier Transform and Mutual Intensity Theory. The integral is oscillatory in value. If there is any stationary phase point, it would be the main contributor to the integral. Equation (4) could also be expressed as

$$\begin{aligned} f(x) = \left(\frac{\mathrm{i}}{\lambda z}\right)^{1/2}\int \exp\{\mathrm{i}k(z+\frac{\mathrm{i}k(x-X)^2}{2z})\} \\ \times \exp\{-k\mu_1 + \mathrm{i}k\varphi_1\}\mathrm{d}X. \end{aligned} \tag{16}$$

where $\mu_1 = \int\limits_z \beta\mathrm{d}z', \varphi_1 = -\int \delta\mathrm{d}z'$. The integral in Eq.(16) can be evaluated approximately using the method of stationary phase.[16] The stationary phase point $(x_\mathrm{s}, y_\mathrm{s})$ is obtained by solving the following equation:

$$x_\mathrm{s} - x + z\varphi_1'(x_\mathrm{s}) = 0. \tag{17}$$

The wave function in the image plane is obtained as follows:

$$f(x) = \sqrt{-\frac{\mathrm{i}}{4+4z\varphi_1''(x_\mathrm{s})}}\exp\{\mathrm{i}k(z + \frac{(x-x_\mathrm{s})^2}{2z} + \varphi_1(x_\mathrm{s})) - k\mu_1(x_\mathrm{s}) - \frac{\pi}{4}\mathrm{i}\}. \tag{18}$$

Then the intensity distribution in the image plane is

$$I = \left|f(x)\right|^2 = \frac{1}{4}\frac{\exp\{-2k\mu_1(x_\mathrm{s})\}}{1+z\varphi_1''(x_\mathrm{s})}. \tag{19}$$

Equation (19) accounts for the effects of both refraction and absorption in object. When the absorption in object can be neglected, the above equation is simplified into

$$I = \frac{1}{4}\left[1 - z\varphi_1''(x_\mathrm{s})\right] = \frac{1}{4}\left[1 - \frac{z\lambda}{2\pi}\varphi''(x_\mathrm{s})\right], \tag{20}$$

which also shows the relation between I and φ.

3. Microfocus phase contrast

So far we have assumed plane-wave incident radiation, which could be obtained by the use of a high-energy synchrotron source or sophisticated x-ray optics. In this case the mechanism of imaging is shown by Eq.(9) in the Fourier form.

In a microfocus-based in-line phase contrast imaging system, which is easier to design and execute in laboratories, plane wave x-rays are replaced by a point source with a finite size (shown in Fig.2). For convenience the source is assumed to be an ideal point source. In practical circumstances an analogous process could be achieved by integrating the point source field over the source region.

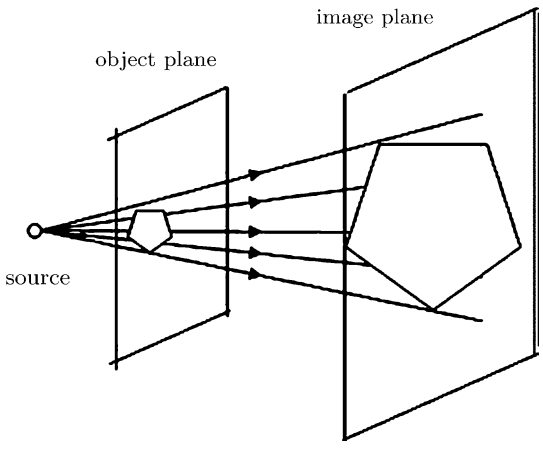


Fig.2. Diagrammatic sketch map of microfocus in-line phase contrast imaging.

According to the theory of Fourier optics,[20] the propagation of a wave in space acts as a kind of linear space filter. The Fresnel integral could be expressed as the convolution of the wavefunction in the starting plane of propagation $f(x_0, y_0)$, which is the same as $f_0(x, y)$, with the space transmission function:

$$f(x, y) = f_0(x, y) * h(x, y), \tag{21}$$

where

$$h(x, y) = \frac{1}{\mathrm{i}\lambda z}\exp\{\mathrm{i}kz\} \times \exp\left\{\frac{\mathrm{i}k}{2z}(x^2+y^2)\right\}. \tag{22}$$

Combining Eq.(21) with Eq.(22), we can obtain the wavefunction after propagation as follows:

$$f(x,y) = \frac{\exp\{\mathrm{i}kz\}}{\mathrm{i}\lambda z}\iint f(x_0,y_0)\exp\left\{\frac{\mathrm{i}k}{2z} \times \left[(x-x_0)^2+(y-y_0)^2\right]\right\}\mathrm{d}x_0\mathrm{d}y_0. \tag{23}$$

This is exactly the same as Eq.(4) in 2-dimensional situation.

In Fourier space, Eq. (21) becomes

$$F(u, v) = F_0(u, v)H(u, v), \tag{24}$$

where

$$H(u, v) = \exp\{\mathrm{i}kz\}\exp\{-\mathrm{i}\pi\lambda z(u^2+v^2)\}. \tag{25}$$

Let us consider a point source. The wavefunction could be expressed as

$$f_0(x,y) = f(x_0,y_0) = \frac{\exp\{\mathrm{i}kr_0\}}{r_0}q(x_0,y_0) \approx \frac{\exp\{\mathrm{i}kR_1\}}{R_1}\exp\left\{\frac{\mathrm{i}k}{2R_1}(x_0^2+y_0^2)\right\} \times q(x_0,y_0). \tag{26}$$

Here the coordinate is chosen so that the point source is located at the origin. R_1 is the distance from the point source to the object plane. Using Eq.(22), the Fourier form of Eq.(26) can be expressed as

$$F_0(u,v) = \mathrm{i}\lambda\exp\{\mathrm{i}kR_1\} \times \exp\{-\mathrm{i}\pi\lambda R_1(u^2+v^2)\} * Q(u,v). \tag{27}$$

Equation (24) then becomes

$$F(u,v) = \mathrm{i}\lambda\exp\{\mathrm{i}kR\}\exp\{-\mathrm{i}\pi\lambda R_1(u^2+v^2)\} * Q(u,v)\cdot\exp\{-\mathrm{i}\pi\lambda z(u^2+v^2)\}, \tag{28}$$

where R is the distance form the source to the image, $R = R_1 + z$. The validity of this expression could be

evaluated when the convolution is expanded into full Fresnel integral, which is the same as the standard result for a spherical-wave source.

Different from Wilkins' argument, in the case of spherical wave incidence the image wavefunction is not a simple replacement of z by $z_{\text{eff}} = R_1 z/(R_1+z)$ in the plane wave condition, and is a much more complicated expression.

4. Experiment

Experiments are carried out using in-line phase contrast method. A Feinfocus FXS 160 whose maximum voltage is 160kV is used as the x-ray source. Its focal size is 5 μm. The sample is suspended by a thread tied to foam, which is laid on a tripod. The centre part of the foam is removed to leave a space for the sample so that x-rays could pass through it without interaction with the foam. Kodak AA400 film is exposed in a precise computer controlled positioning system, then scanned and digitized by an IMACON848 scanner. In the whole experimental process the tube voltage is set at 30 kV and the current at 200 μA. The experimental system is shown in Fig.3.

The sample used is a dead ant dried for 5 days so that its water effect can be neglected in experiment. In this case absorption is minor, which creates a better environment for using phase contrast. The size of the ant is 5 mm × 10mm, with a thickness of 4mm or so. In order to examine the differences between various imaging positions, the object film distance (OFD) is changed with a constant magnification of 6. The x-ray exposure time is selected such that all the images on the film have the same optical density.

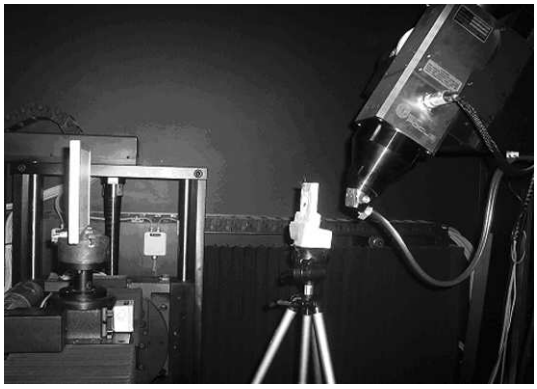


Fig.3. Experimental system.

5. Results and discussion

To investigate the effect of imaging position on the phase-contrast image we perform the experiments at source object distances (SODs) ranging from 4 cm to 9 cm. When SOD is 4 cm, the corresponding OFD is 20 cm, which could be considered as a short distance. The image taken here has more absorption information than that taken at a greater distance. Pure absorption images are not taken for two reasons. One is that it requires OFD to be zero, which corresponds to zero magnification. Therefore, a comparison between it and a magnified image is meaningless. The other is that in this case, part of the sample in the image would be too small to extract valuable information. Images taken separately at SODs of 4 cm and 9 cm, which includes more phase contrast effects, are compared in Fig.4.

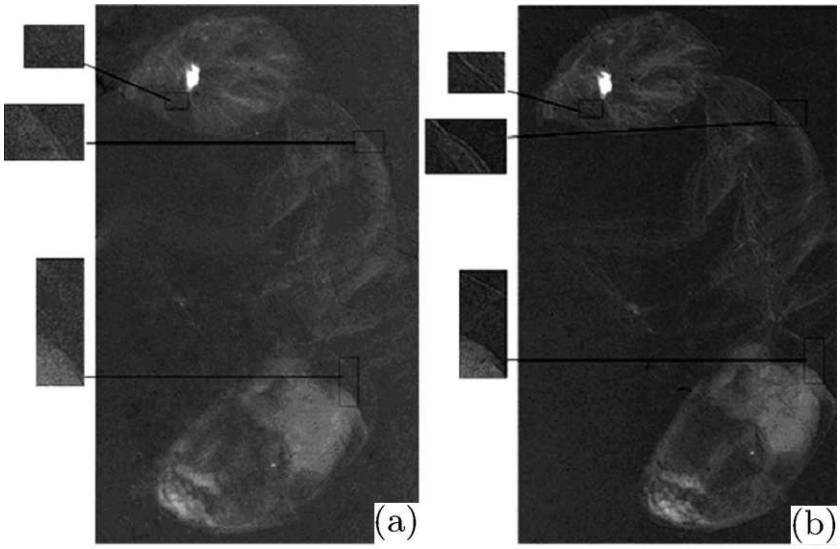


Fig.4. Comparison between images at different positions. (a) SOD is 4 cm; OFD is 20 cm. (b) SOD is 9 cm; OFD is 45cm.

From these two images it is clear that the image including more phase contrast effects is better in image quality. First, the contrast is much better. The forelimb of the ant can be clearly seen in Fig.4(b) while it is not discernable in Fig.4(a) which does not contain so many phase contrast effects. Second, the resolution is improved. Three parts of the images are compared: head, back and stomach. For the head, the detail of intercrossing nerve fibres is shown in Fig.4(b) while they are blurred in Fig.4(a). For the back, the interface between air and ant is much clearer in Fig.4(b), which could be interpreted based on the theory presented in Section 2. Those x-ray beams refract when there exists any density variation in the material. Thus in Fig.4.(b), where the phase effect is more prominent, the x-ray beam shifts toward the direction of the ant's body and only a small amount of x-rays scattered on the edges of its body arrives at the interface. Therefore, the film is underexposed and a clear white interface is generated. A comparison between stomach images is based on the same explanation, from which the Laplacian relationship mentioned above is demonstrated. In order to investigate quantitatively the influence of imaging position on in-line phase contrast, the edge contrasts of all 6 images are compared. Edge contrast is considered to be $C = \dfrac{I_{\rm out} - I_{\rm in}}{I_{\rm out}}$, where $I_{\rm out}$ and $I_{\rm in}$ refer to the image intensities outside and inside the interfaces, respectively. The area to be investigated is the stomach of the ant, where edge contrast is most prominent. Figure 5 shows the difference in edge contrast among various SOD.

The improvement on edge contrast is observed with the increase of SOD. However, a very long SOD is impractical as the corresponding OFD would cause a too long exposure time due to the low current used in the microfocus mode.

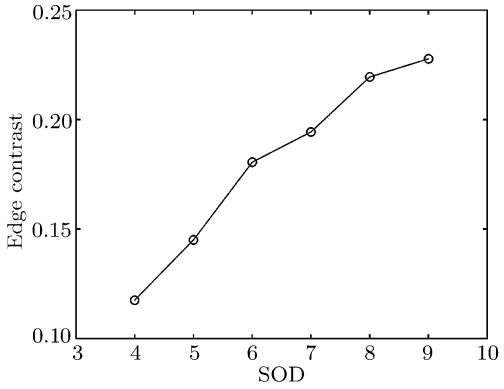


Fig.5. Edge contrast of images at different positions. The projection magnification is kept constant at 6 and the exposure time is controlled to remain at the same optical density.

6. Conclusions

In this paper the basic principles of in-line phase contrast are reviewed, especially the important relationship between the intensity distribution in the image plane and the Laplacian of phase shift. In the situation of a microfocus x-ray source, the Fourier form is suggested and demonstrated. The enhancement of Phase contrast image is observed, and the edge contrasts of images at different imaging positions are compared. The results show that the phase contrast technique has a potential of improving contrast and resolution for weakly absorbing materials, including corrosion, cracks, blebs and interfaces. The technique could be applied in biomedical engineering, material engineering and nuclear engineering.

Although various phase contrast techniques have emerged in recent years, much work remains to be done either on the improvement of phase contrast theory or on its applications. Our future work will focus on phase contrast tomography and its application to larger samples.

References

[1] Zernike 1935 *Physik* **16** 454
[2] Gabor D 1948 *Nature* **161** 777
[3] Schmahl G, Rudolph D, Guttmann P, Schneider G, Thieme J, Niemann B and Wilhein T 1994 *Synchrotron Radiation News* **7** 19
[4] Palmer J R and Morrison G R 1992 *X-ray Microscopy* III **67** 278
[5] Morrison G R 1993 in *Proceedings of the 4th International Conference* p20
[6] Momose A 1995 *Nucl. Instrum. Meth. Phys. Res.* A **352** 622
[7] Davis T J, Gao D, Gureyev T E, Stevenson A W and Wilkins S W 1995 *Nature* **373** 595
[8] Davis T J, Gureyev T E, Gao D, Stevenson A W and Wilkins S W 1995 *Phys. Rev. Lett.* **74** 3173
[9] Chapman D, Thomilinson W, Arfelli F, N Gm ü r, Zhong Z, Menk R, Johnston R E, Washburn D, Pisano E and Sayers D 1995 *Rev. Sci. Instrum.* **66** 1329
[10] Chapman D, Thomlinson W, Johnston R E, Washburn D, Pisano E, Gmür N, Zhong Z, Menk R, Arfelli F and Sayers D 1997 *Phys. Med. Biol* **42** 2015
[11] Wilkins S W, Gureyev T E, Gao D, Pogany A and Stevenson A W 1996 *Nature* **384** 335

[12] Snigirev A, Snigireva I, Kohn V, Kuznetsov S and Schelokov I 1995 *Rev. Sci. Instrum.* **66** 5486

[13] Cloetens P, Barrett R, Baruchel J, Guigay J P and Schlenker M 1996 *J. Phys. D: Appl. Phys.* **29** 133

[14] Pogany A, Gao D and Wilkins S W 1997 *Rev. Sci. Instrum.* **68** 2774

[15] John M C 1995 *Diffraction Physics* 3rd ed (Amsterdam: North Holland) pp11-17

[16] Born M and Wolf E 1999 *Principles of optics* (New York: Cambridge University Press) p888

[17] Jing Cheng and Han S 1999 *Optics Communications* **172** 17

[18] Gureyev T E and Wilkins S W 1998 *J. Opt. Soc. Am.* A **15** 579

[19] Mayo S C, Miller P R, Wilkins S W, Davis T J, Gao D, Gureyev T E, Paganin D, Parry D J, Pogany A and Stevenson A W 2002 *J. Microscopy* **207** 79

[20] Goodman J W 2005 *Introduction to fourier optics* (San Francisco: McGraw-Hill) p67